Modeling of Adsorption Dynamics at Air-Liquid Interfaces Using Statistical Rate Theory (SRT)

Mohammad Elias Biswas, Ioannidis Chatzis, Marios A. Ioannidis and Pu Chen

Department of Chemical Engineering,University of Waterloo, Waterloo, Ontario, Canada N2L 3G1

Abstract: A large number of natural and technological processes involve mass transfer at interfaces. Interfacial properties, e.g., adsorption, play a key role in such applications as wetting, foaming, coating, and stabilizing of liquid films. The mechanistic understanding of surface adsorption often assumes molecular diffusion in the bulk liquid and subsequent adsorption at the interface. Diffusion is well described by Fick's law, while adsorption kinetics is less understood and commonly described using Langmuir-type empirical equations. In this study, a general theoretical model for adsorption dynamics at the air-liquid interface is developed where a new kinetic equation based on the Statistical Rate Theory (SRT) is derived. The present model of adsorption dynamics is governed by three dimensionless numbers: ψ (ratio of adsorption thickness to diffusion length), λ (ratio of square of the adsorption thickness to the ratio of adsorption to desorption rate constant), and N_k (ratio of the adsorption rate constant to the product of diffusion coefficient and bulk concentration). Numerical simulations for surface adsorption using the proposed model are carried out. The difference in surface adsorption between the general and the diffusion controlled model is estimated and presented graphically as contours of deviation. Three different regions of adsorption dynamics are identified: diffusion controlled (deviation less than 10%), mixed-diffusion-transfer controlled (deviation in the range of 10 – 90%), and transfer controlled (deviation more than 90%). These three different modes predominantly depend on the value of N_k. The corresponding ranges of N_k for the studied values of ψ ($10^{-2}<\psi<10^{4}$) and λ ($10^{-12}<\lambda<10^{8}$) are: $10^{1}<N_k<10^{4}$ for the diffusion controlled, $10^{-3}<N_k<10^{1}$ for the mixed-diffusion-transfer controlled, and $10^{-4}<N_k<10^{-3}$ for the transfer controlled, respectively.

1. Introduction

The surface tension of a freshly formed interface of any solution containing a surface active component is very close to that of the pure solvent. With time, the surface tension decreases as the surface active component adsorbs at the interface. This time dependent surface tension is known as the dynamic surface tension (DST). The dynamic surface tension is an important property; it governs many interfacial processes of practical interest [1-2], including wetting, foaming, coating, stabilizing of liquid films [3], enhanced oil recovery [4], breathing [5-6], nerve conduction, and transfer across cell membranes [5].

Since the pioneer work of Ward and Tordai [7] in the 1940s, the kinetics of adsorption at the interface has been a focus of surface science research [8-10]. It is well known that the adsorption of a component from a liquid bulk phase to an air-liquid interface generally includes three steps: (i) transport of the component from the bulk phase to the "subsurface", immediately adjacent to the interface (surface); (ii) transfer of the component from the subsurface to the surface; and (iii) rearrangement of the adsorbed component into an equilibrium state [8]. The rate-determining step for adsorption can be either one of the above three steps. Accordingly, the adsorption kinetics is said to be diffusion controlled, transfer

controlled or rearrangement controlled, depending on whether step (i), (ii) or (iii) is the rate limiting step, respectively. The adsorption kinetics is mixed-diffusion-transfer controlled when steps (i) and (ii) are equally important. Currently, most of the theoretical models have been developed using the following two mechanisms: diffusion controlled [9-12] and mixed-diffusion-transfer controlled [13-17]. Rearrangements at the surface may consist of reorientation, conformational changes, complex formation, chemical reactions, phase transitions or formation of three-dimensional structures resembling liquid crystals. For small molecules, rearrangement is generally a very fast process and has little effect on the overall behavior of adsorption [5, 18].

The diffusion controlled model of adsorption dynamics is often used for the description of the dynamic surface tension data, which are often obtained by measuring surface tension with a pendant drop (or bubble). The solution of Ward and Tordai for diffusion controlled adsorption was developed for a planar interface. An analogous solution was obtained by Lin et al. [13], where adsorption to a bubble was considered and the bubble shape was approximated as a spherical interface. Ferri et al. [12] reported that the geometry of the interface significantly affects the adsorption. Adsorption to a spherical interface is faster than that of a planar interface for a bubble, whereas, for a pendant drop, the adsorption to a spherical interface is slower than that of a planar interface [13, 19].

The transfer process, i.e., step (ii) above, is important when a sufficiently large activation energy exists [19]. In such cases the mixed-diffusion-transfer controlled model must be considered, and hence an appropriate transfer kinetic equation is necessary [19]. Most of the kinetic equations used were based on the Arhenius rate formulation using an activation energy. These equations are empirical, and the constants involved are evaluated by fitting to experimental data. There are considerable uncertainties in the estimating of these empirical constants [19]. Although these equations can be used by adjusting the empirical parameters or adding more empirical parameters in describing transfer kinetics, the research thrust in obtaining a better transfer equation based on the first physical principles was pinpointed. The transfer equation based on the Statistical Rate Theory (SRT) has been developed by Chen & Neumann [20]. The SRT is based on quantum mechanics and thermodynamics. The SRT transfer equation involves less empirical assumptions, and the rate constants can be evaluated from the theory.

The overall objective of this paper is to formulate a general model for adsorption of molecules at the air-liquid interface. Both diffusion in the liquid bulk and transfer at the surface are considered. The transfer equation is derived based on SRT, which is a modification of Chen & Neumann's equation [20]. The paper is structured as follows: Section 2 describes the theoretical aspects of diffusion and the transfer kinetic process. In Section 3, the governing equations for adsorption dynamics are written in dimensionless form. The approach to the numerical solution is also discussed. Section 4 discusses the simulation results from both the diffusion controlled and the mixed-diffusion-transfer controlled model. Key conclusions are summarized in Section 5.

2. Theoretical aspects

The adsorption of molecules from a liquid bulk to an air-water interface is modeled using a two-step process: diffusion of the molecules from the bulk to the sub-surface, and transfer of the molecules from the sub-surface to the air-water interface. Since for many small molecules, rearrangement at the surface is fast, possible effects of step 3 on the overall adsorption are ignored here.

2.1 Diffusion equation

One-dimensional diffusion of the molecules from the bulk of the pendant drop to the sub-surface is assumed. The bulk liquid contains a surface active material with a uniform initial concentration. The geometry of the pendant drop is approximated as a sphere. The diffusion is assumed to be spherically symmetrical and is described by the Fick's second law [14-17]:

$$\frac{\partial C}{\partial t} = \frac{D}{r^2}\frac{\partial}{\partial r}\left(r^2 \frac{\partial C}{\partial r}\right) \tag{1}$$

with the following boundary and initial conditions:

$$\text{at} \quad r = 0, \quad \frac{\partial C}{\partial r} = 0$$

$$\text{at} \quad r = r_s, \quad -D\frac{\partial C}{\partial r}\Big|_{r=r_s} = \frac{\partial \Gamma}{\partial t} \tag{2}$$

at t = 0, $C = C_o$ and $\Gamma = \Gamma_o$

where r is the spherical radial coordinate, t the time, D the diffusion coefficient, C the bulk concentration, Γ the surface concentration, r_s the drop radius, C_o the initial bulk concentration, and Γ_o the initial surface coverage. Ideally, for a fresh pendant drop the initial surface coverage should be zero; however, during the creation of the drop a small amount of molecules may appear at the surface.

2.2 Transfer equation

To complete the description of the model, the transfer of molecules from the sub-surface to the surface must be specified. The transfer equation derived from the Statistical Rate Theory (SRT) for ideal surface condition is given in [19, 22, 25].

The general form of the kinetic equation derived from the Statistical Rate Theory (SRT) can be written as follows:

$$J = \frac{d\Gamma}{dt} = k_a \frac{f^V}{f^A}\frac{C_s}{\Gamma}\exp\left(-\frac{\pi}{kT\Gamma_\infty}\right) - k_d \frac{f^A}{f^V}\frac{\Gamma}{C_s}\exp\left(\frac{\pi}{kT\Gamma_\infty}\right) \tag{3}$$

where k_a and k_d are the adsorption and the desorption rate constant, respectively, f^V and f^A are the activity coefficients of the bulk and the surface, respectively, C_s is the sub-surface concentration, Γ_∞ is the maximum surface concentration, k is the Boltzmann constant, T is the temperature, and π is the surface spreading pressure, defined as $\pi=\gamma_o-\gamma$, where γ_o and γ are the solvent and solution surface tensions, respectively.

For a surfactant molecule below its critical micelle concentration, the bulk solution can be approximated as ideal and hence f^V is considered as unity and Eq (3) becomes,

$$J = \frac{d\Gamma}{dt} = k_a \frac{C_s}{f^A \Gamma} \exp\left(-\frac{\pi}{kT\Gamma_\infty}\right) - k_d \frac{f^A \Gamma}{C_s} \exp\left(\frac{\pi}{kT\Gamma_\infty}\right) \quad (4)$$

Equation (4) is an implicit transfer kinetic equation with respect to the surface concentration because surface spreading pressure is also a function of surface concentration. In order to obtain an explicit transfer kinetic equation, a surface equation of state that relates surface pressure to surface concentration and an expression for the surface activity coefficient are needed. Equation (4) is a general kinetic equation and is valid for both ideal and non-ideal surfaces. For non-ideal surfaces an expression for surface activity coefficient is required. For an ideal surface the surface activity coefficient is taken to be unity and Equation (4) becomes,

$$J = \frac{d\Gamma}{dt} = k_a \frac{C_s}{\Gamma} \exp\left(-\frac{\pi}{kT\Gamma_\infty}\right) - k_d \frac{\Gamma}{C_s} \exp\left(\frac{\pi}{kT\Gamma_\infty}\right) \quad (5)$$

Equation (5) is the SRT kinetic equation for an ideal surface. In order to solve this transfer kinetic equation, a surface equation of state that relates surface pressure to surface concentration is needed. One of the extensively used surface equations of state is as follows [2, 7]:

$$\pi = -\Gamma_\infty kT \ln\left(1 - \frac{\Gamma}{\Gamma_\infty}\right) \quad (6)$$

Substitution of Equation (6) into Equation (5) gives

$$J = \frac{d\Gamma}{dt} = k_a \left[\frac{C_s}{\Gamma}\left(1 - \frac{\Gamma}{\Gamma_\infty}\right) - \frac{1}{K}\frac{\Gamma}{C_s}\left(\frac{1}{1 - \Gamma/\Gamma_\infty}\right)\right] \quad (7)$$

where $K = k_a/k_d$

Equation (7) is the final form of the transfer kinetic equation based on the Statistical Rate Theory. This equation consists of two parts: adsorption and desorption. The adsorption is directly proportional to the bulk concentration and the available empty sites at the interface, but inversely proportional to the surface concentration. The desorption is inversely proportional to the bulk concentration and the available empty sites at the interface, but directly proportional to the surface concentration. The adsorption and desorption rate constants of Equation (7) are not empirical and can be estimated from independent theoretical considerations, as detailed elsewhere [20, 22].

At equilibrium, when the rate of change in surface concentration vanishes, any transfer kinetic equation should appropriately reflect an equilibrium isotherm. This is illustrated by setting J=0 in Eq. (7) and the equilibrium isotherm becomes,

$$\frac{\Gamma}{\Gamma_\infty} = \frac{C}{b+C} \quad \textit{where } \mathrm{b} = \Gamma_\infty \sqrt{\mathrm{k_d}/\mathrm{k_a}} \tag{8}$$

Equation (8) is the Lamgmuir type isotherm where b is the equilibrium constant. It is thus interesting to note that although the transfer kinetic equation, Eq. 7, is completely different from the Langmuir type kinetic equation, the two isotherms are the same.

3. Dimensionless equations and numerical schemes

3.1 Dimensionless equations

For convenience in mathematical treatments and numerical solutions, the governing equations have been rewritten in terms of dimensionless parameters:

$$C^* = \frac{C}{C_0}, \xi = \frac{r}{r_s}, \Gamma^* = \frac{\Gamma}{\Gamma_\infty}, \tau = \frac{tD}{h^2} \tag{9}$$

where C^* is the dimensionless concentration, ξ the dimensionless distance, Γ^* the dimensionless surface concentration, τ the dimensionless time, and h defined as Γ_∞/C_0.
Thus Eq. (1) becomes

$$\frac{\partial C^*}{\partial \tau} = \psi^2 \left[\frac{\partial^2 C^*}{\partial \xi^2} + \frac{2}{\xi}\frac{\partial C^*}{\partial \xi} \right] \text{ where } \psi \equiv \frac{h}{r_s} \tag{10}$$

The B.C., Eq. (2), becomes:

at $\xi = 0, \ \dfrac{\partial C^*}{\partial \xi} = 0$ (11)

at $\xi = 1, \ -\dfrac{\partial C^*}{\partial \xi}\Big|_{\xi=1} = \dfrac{1}{\psi}\dfrac{\partial \Gamma^*}{\partial \tau}$ (12)

The transfer kinetic Equation (7) becomes

$$\frac{d\Gamma^*}{d\tau} = N_k \left[\frac{C_S^*}{\Gamma^*}\left(1-\Gamma^*\right) - \lambda \frac{\Gamma^*}{C_s^*}\left(\frac{1}{1-\Gamma^*}\right) \right] \tag{13}$$

where $\lambda \equiv h^2/K$ and $N_k \equiv k_a/DC_o$ (14)

The equilibrium isotherm Eq. (8) becomes

$$\Gamma^* = \frac{C^*}{\alpha + C^*} = \frac{C^*}{\sqrt{\lambda} + C} \tag{15}$$

where $\alpha=b/C_o$ and $\lambda=\alpha^2$

The non-dimensional equations (10) and (13) involve three dimensionless numbers $\psi\equiv h/r_s$, ((h2/K, and Nk(ka/DCo. The physical significance of each of these dimensionless numbers is given in [22]. Ranges of each of the dimensionless numbers are shown in Table 1.

Table-1: Ranges of three dimensionless numbers

Parameter	Lower limit	Upper limit
(	1.0x10-5	**$1.0x10^{5}$**
λ	**$1.0x10^{-14}$**	**$1.0x10^{10}$**
N_k	**$1.0x10^{-5}$**	**$1.0x10^{6}$**

3.2 Numerical solution methods

When the overall adsorption process is controlled by bulk diffusion, the surface concentration can be obtained by solving Eq. (10) and Eq. (15). In this case, $N_k \rightarrow \infty$, and the entire adsorption dynamics is described by two dimensionless numbers, ψ and λ. If the adsorption process is mixed-diffusion-transfer controlled, Eq. (10) and Eq. (13) need to be solved simultaneously to obtain the surface concentration. In the mixed-diffusion-transfer model the dynamics is described by all three dimensionless numbers, ψ, λ, and N_k.

Equations 10-15 are inhomogeneous and nonlinear, precluding an analytical solution. It is thus necessary to employ numerical methods to solve the system of equations. Different numerical techniques, including integral, finite difference and finite element methods, have been reported in the literature [11-13, 19]. The numerical package gPROMS (Process Systems Enterprise Ltd.,UK) has been used for the simulation [24]. Details of the numerical methods were given in [22].

The numerical simulation is carried out in the following sequence: (i) First, a detailed simulation is carried out by varying the dimensionless numbers (ψ, λ) within the regime of the diffusion controlled dynamics (e.g., $N_k \rightarrow\infty$); (ii) Second, a detailed simulation is carried out by varying all three dimensionless numbers (ψ, λ and N_k) for the case of mixed-diffusion-transfer model; (iii) Finally, the difference between results of the mixed-diffusion-transfer and the diffusion controlled model is calculated.

4. Results and discussion

4.1 Effect of dimensionless parameter

Effect of ψ: Figure 1 shows the dimensionless surface concentration plotted against the dimensionless time for a wide range of ψ at a constant value of $\lambda=10^{-6}$. Figure 1

represents one of the many similar plots obtained from the detailed simulations for the diffusion controlled model. The plots in Figure 1 show that the surface concentration increases with decreasing the value of ψ at a constant value of λ. When ψ is decreased to 10^{-2}, surface adsorption reaches a maximum (curve d) and a further decrease of ψ to 10^{-3} (curve e) does not increase the surface concentration further. This indicates that the effect ψ on surface adsorption is negligible for ψ below 10^{-2}. Similar effects of ψ on surface adsorption are found for all other values of λ.

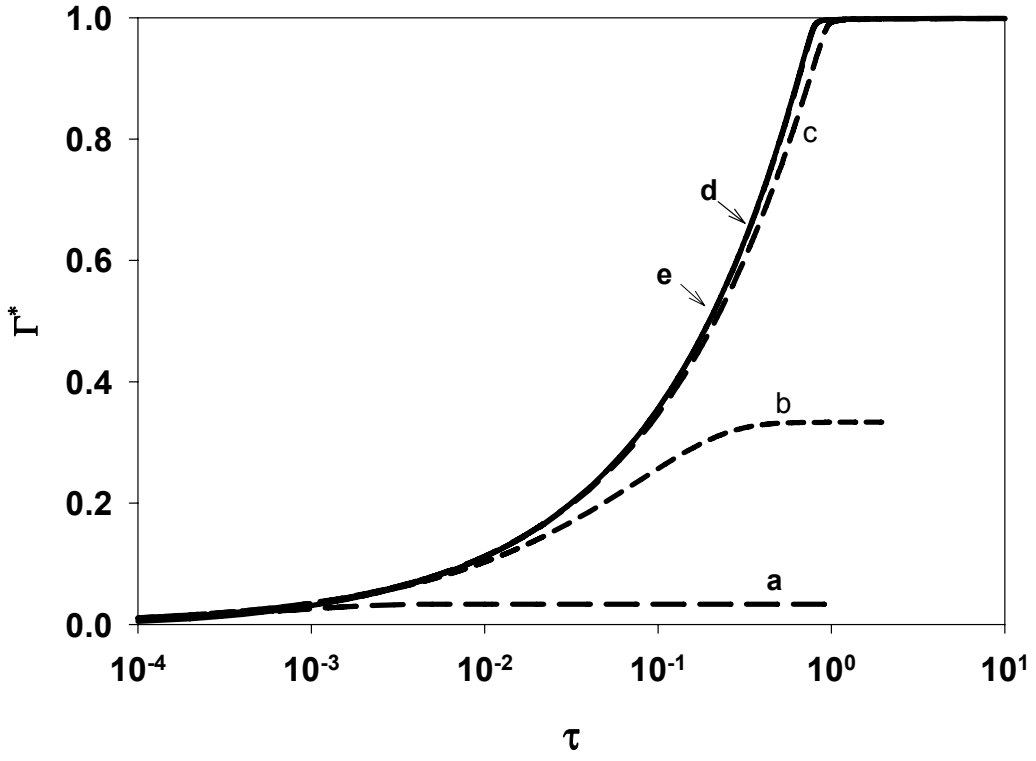

Figure 1 Evolution of dimensionless surface concentration with dimensionless time for diffusion controlled dynamics at a constant $\lambda=10^{-6}$ for various values of (a) $\psi = 10^{1}$, (b) $\psi =$ 1.0, (c) $\psi = 10^{-1}$, (d) $\psi=10^{-2}$, and (e) $\psi =10^{-3}$.

Effect of λ: Figure 2 plots the dimensionless surface adsorption against the dimensionless time for different values of λ at a constant value of $\psi=10^{-1}$. Similar plots are obtained from the simulations for other values of ψ. It is observed in Figure 2 that decreasing λ increases the surface adsorption. This increase in equilibrium surface adsorption is due to the higher equilibrium adsorption constant (K). In Figure 2, the surface adsorption reaches a maximum when λ attains a value of 10^{-8} (curve g). Below this value of λ, further decrease in λ does not change the surface adsorption. This is shown in curves g, h and i corresponding to λ equal to 10^{-8}, 10^{-10}, and 10^{-12}, respectively, in Figure 2, where these curves are indistinguishable. The value of λ below which no further increase in surface adsorption occurs differs for different values of ψ.

Figures 1 and 2 reveal that the surface concentration increases with time towards a plateau value. The magnitudes of surface concentrations at the plateau are taken as the equilibrium surface concentrations. The equal surface concentration for a particular value of ψ can be obtained from different values of λ. Among these series of λ values, one can use any value of λ to obtain the same maximum surface concentration at a particular ψ. As mentioned earlier, the decrease in λ increases the surface concentration, and there is a limiting λ value below which surface concentration does not increase further.

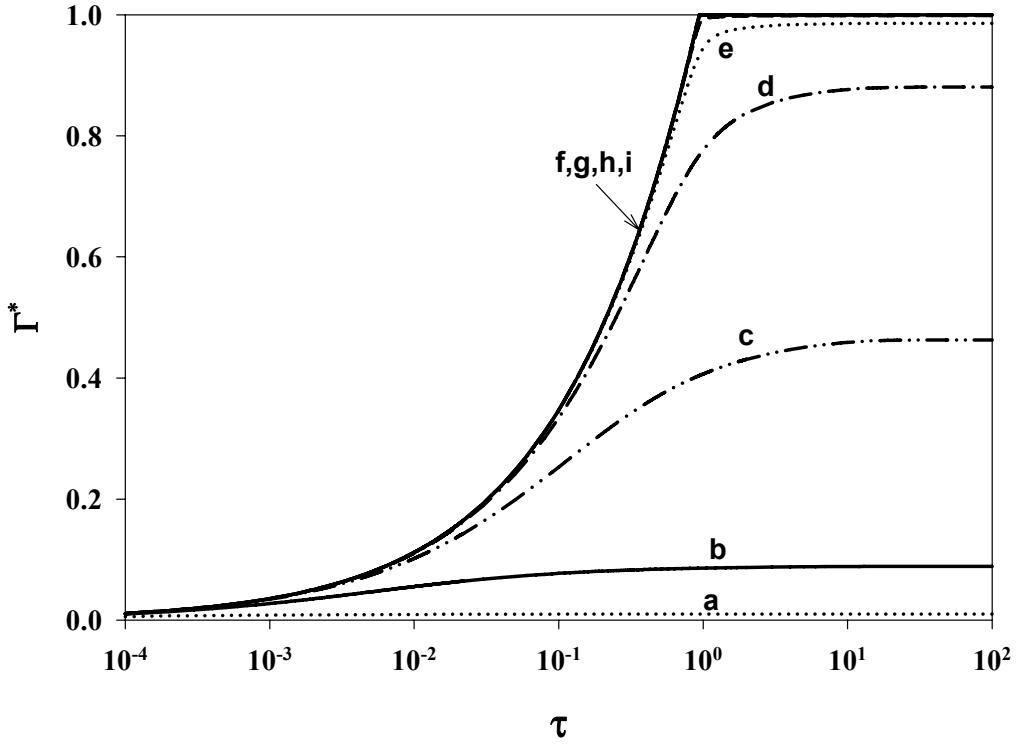

Figure 2 Evolution of dimensionless surface concentration with dimensionless time for diffusion controlled dynamics at a constant $\psi=10^{-1}$ for various values of (a) $\lambda=10^{4}$, (b) $\lambda=10^{2}$, (c) $\lambda=1.0$, (d) $\lambda=10^{-2}$, (e) $\lambda=10^{-4}$, (f) $\lambda=10^{-6}$, (g) $\lambda=10^{-8}$, (h) $\lambda=10^{-10}$, and (i) $\lambda=10^{-12}$.

4.2 Simulation of adsorption dynamics using the mixed-diffusion-transfer model

Numerical solutions to the mixed-diffusion-transfer model have been reported in the literature where a diffusion equation and an empirical Langmuir type kinetic equation were used [2, 11, 14-17, 23, 25-26]. In all cases, experimental surface tension data were fitted to the model by adjusting fitting parameters. However, in the present study, numerical simulations are carried out in terms of the three dimensionless numbers. Values of these

dimensionless numbers for different modes of adsorption kinetics can be obtained from a given experimental system.

As mentioned earlier, the mixed-diffusion-transfer controlled model requires specification of all 3 dimensionless numbers for describing the adsorption dynamics. Like the diffusion controlled model where simulations are carried out by varying one dimensionless number while fixing the other, the simulation of the mixed-diffusion-transfer model are carried out by fixing two numbers (ψ and λ) while varying the third number (N_k).

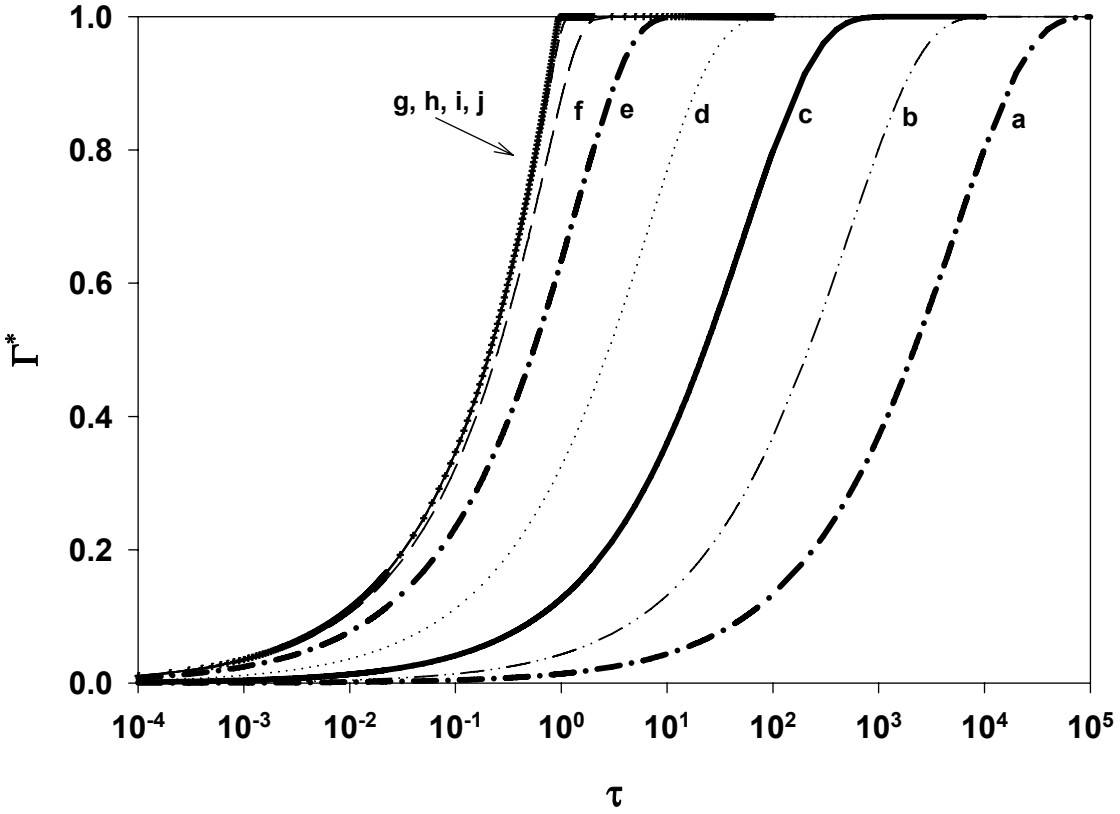

Figure 3 Evolution of dimensionless surface concentration with dimensionless time for mixed-diffusion-transfer controlled adsorption dynamics at constant values of $\psi=10^{-1}$ and $\lambda=10^{-8}$, for various values of N_k (a) $N_k=10^{-4}$, (b) $N_k=10^{-3}$, (c) $N_k=10^{-2}$, (d) $N_k=10^{-1}$, (e) $N_k=1.0$, (f) $N_k=10^{1}$, (g) $N_k=10^{2}$, (h) $N_k=10^{3}$, (i) $N_k=10^{4}$, and (j) diffusion-controlled result ($N_k=\infty$).

Figure 3 is one of the typical results, where the dimensionless surface concentration is plotted against the dimensionless time for fixed values of $\psi=10^{-1}$ and $\lambda=10^{-8}$ but different values of N_k. In the same graphs, the result for the diffusion controlled model ($N_k\rightarrow\infty$) using the same values of ψ and λ is plotted for comparison. Figure 3 shows that the dynamics of surface adsorption is accelerated as N_k increases. As mentioned earlier, an increase in N_k

means an increase in adsorption rate constant, k_a, at constant ψ and λ, and hence speeding up of the adsorption process. Figure 3 also reveals that when N_k becomes larger than 100, the curves of dimensionless surface adsorption (curves g, h and i) become indistinguishable from that of the diffusion controlled case (curve j). It is observed that although the upper range of N_k is estimated to be 10^6 in Table-1, in practice, the surface concentration coincides with that of the diffusion-controlled when N_k is equal to or greater than 10^2 at $\psi=10^{-1}$ and $\lambda=10^{-8}$.

4.3 Comparison between the mixed-diffusion-transfer model and the diffusion controlled model

Calculation of deviations: The surface concentration obtained from the solution to the mixed-diffusion-transfer model is compared, at each time, with that of the diffusion controlled model. For each pair of ψ and λ, N_k varies over its entire range of values. The deviation of the mixed-diffusion-transfer model solution from the diffusion controlled for a fixed pair of ψ and λ is computed as a function of dimensionless time. The computed deviation is then normalized using the equilibrium dimensionless surface concentration of the diffusion controlled solution. The maximum normalized deviation can be calculated through the following equation:

$$d(N_k,\psi,\lambda) = \mathrm{Max}\left[\frac{\Gamma_i^*(\psi,\lambda,\tau_i) - \Gamma_i^*(N_k,\psi,\lambda,\tau_i)}{\Gamma_{eq}^*(\psi,\lambda)}\right] * 100 \qquad (16)$$

where $d(N_k,\psi,\lambda)$ is the percent deviation at fixed values of ψ, λ and N_k, i denotes a point in dimensionless time, and $\Gamma_{eq}^*(\psi,\lambda)$ is the equilibrium surface concentration for fixed values of ψ and λ Table 2 lists typical results from Eq. 16.

Table-2: Estimated maximum percent deviations at $\psi=10^{-1}$ as a function of N_k and λ

λ \ N_k	10^4	10^3	10^2	10^1	1	10^{-1}	10^{-2}	10^{-3}	10^{-4}
10^{-12}	0.2024	0.9384	3.9037	14.0492	38.1139	68.3146	87.6778	95.7952	98.6354
10^{-10}	0.1406	0.8693	3.8344	13.9801	38.0450	68.2461	87.6174	95.7753	98.6198
10^{-8}	0.0564	0.5996	3.5316	13.6773	37.7453	67.9938	87.4484	95.6535	98.5398
10^{-6}	0.0223	0.2264	2.4166	12.4234	36.4975	66.9070	86.6682	95.1464	98.2277
10^{-4}	0.0078	0.0783	0.8367	8.1734	31.8817	62.8213	83.7604	93.3593	97.2176
10^{-2}	0.0049	0.0252	0.2510	2.6773	19.8628	51.2375	75.5771	88.6908	95.0140
1	0.0007	0.0084	0.0860	0.8831	8.3813	33.5028	61.2735	80.0232	90.6497
10^2	0.0006	0.0053	0.0528	0.5375	5.2266	24.5493	50.8960	71.5231	84.3796
10^4	0.0076	0.8302	0.0503	0.4974	4.8232	23.0883	48.9071	69.4887	82.5604
10^6	0.1407	0.1409	0.1435	0.4485	3.8774	22.0978	49.1380	69.4065	82.3517
10^8	0.8826	0.8835	0.8922	0.9784	1.8321	10.8758	38.2093	66.3650	83.7471

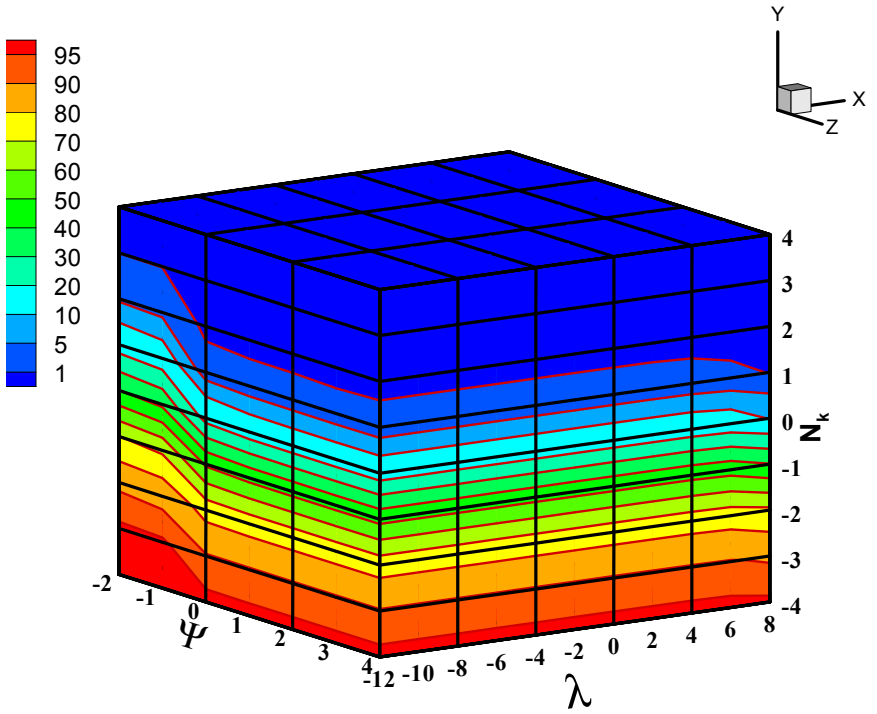

(A)

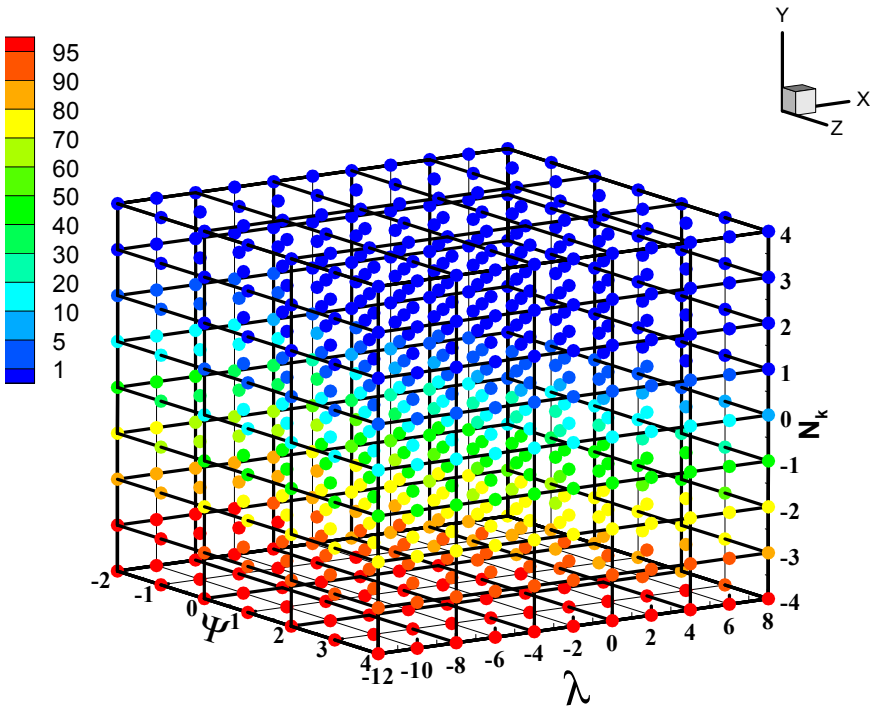

(B)

Figure 4 Three dimensional contours of normalized deviation showing all three dimensionless numbers (A) continuous volume plot (B) scatter plot.

3-D contours: Figure 4(a) shows a 3-dimensional volume contour plot of the percent deviation. The X, Y and Z coordinates represent the three independent parameters λ, N_k, and ψ, respectively, in log scales. The color code represents the percentage of deviation, varying from blue (less than 5%) to red (more than 90% deviation). Figure 4(b) gives the scatter plot of Figure 4(a). It is shown that for all values of ψ and λ, the deviation is low at high N_k values, and high at low N_k values. This reveals that N_k is a predominant number. Figure 4 identifies different regions of the adsorption dynamics using the following criteria: diffusion-controlled if the deviation is less than 10%; mixed-diffusion-transfer controlled if the deviation is between 10 and 90%; and transfer-controlled if the deviation is more than 90%. Accordingly, it can be found that the dynamics becomes diffusion controlled for $10^{1}<N_k<10^{4}$, mixed-diffusion-transfer controlled for $10^{-3}<N_k<10^{1}$, and transfer controlled for $10^{-4}<N_k<10^{-3}$, for all values of ψ ($10^{-2}<\psi<10^{4}$), and λ ($10^{-12}<\lambda<10^{8}$).

5. Conclusions

- A mathematical model for adsorption from a liquid solution to an air-water interface was developed, where the transfer kinetic equation was based on the Statistical Rate Theory (SRT). This kinetic equation has a different functional form than those of the literature reported kinetic equations.
- The model was described using three dimensionless numbers ψ (ratio of adsorption thickness to diffusion length), λ (ratio of square of the adsorption thickness to the ratio of adsorption to desorption rate constant), and N_k (ratio of the adsorption rate constant to the product of diffusion coefficient and bulk concentration).
- Increase in surface adsorption and consequently reduction in surface tension is maximum for low values of ψ and λ. The limiting value of ψ, below which surface adsorption does not increase further, is 10^{-2} for $10^{-12}<\lambda<10^{8}$.
- Deviations between the solution to the mixed-diffusion-transfer and the diffusion controlled model were calculated and presented as contour plots. Three different regions of adsorption dynamics were identified: diffusion controlled (deviation less than 10%) for $10^{1}<N_k<10^{4}$, mixed-diffusion-transfer controlled (deviation in between 10 – 90%) for $10^{-3}<N_k<10^{1}$, and transfer controlled (deviation more than 90%) for $10^{-4}<N_k<10^{-3}$, respectively, for all ψ ($10^{-2}<\psi<10^{4}$), and λ ($10^{-12}<\lambda<10^{8}$).
- The modes of adsorption kinetics can be predicted predominantly by estimating the magnitude of N_k. This can be very useful in designing an experiment of a particular kinetics.

References

[1] F. Ravera, M. Ferrari, L. Liggieri. Adv. Colloid and Interface Sci. 88 (2000) 129.
[2] J. Eastoe, J.S. Dalton, Adv. in Colloid and Interface Sci. 85 (2000) 103.
[3] H. Diamant, G. Ariel, D. Andelman. Colloids and Surfaces-A. 183-185 (2001) 259.
[4] R. Miller, R. Sedev, K.-H. Schano, C. Ng, A.W. Naumann, Colloids and Surfaces 69 (1993) 209.

[5] M. van den Tempel, E.H. Lucassen-Reynders, Adv. Colloid and Interface Sc. 18 (1983) 281.
[6] S.Y. Park, R.E. Hannemann, E.I. Franses, Colloids and Surfaces B: 15 (1999) 325.
[7] A. F. H. Ward, J. Tordai. J. Chem. Phys. 14 (1946) 453.
[8] S.S. Dukhin, G. Kretzschmar, R. Millar, in: D. Möbius, R. Miller (Eds.), Dynamics of Adsorption at Liquid Interfaces: Theory, Experiment, Applications, Studies in Interface Science Series, Elsevier, Amsterdam. 1995.
[9] R.P. Borwankar, D.T. Wasan. Chemical Engineering Sci. 43 (1988) 1323.
[10] G. Miller, G. Kretzchmar. Adv. Colloid Interface Sci. 37 (1991) 97.
[11] Y.-C.Liao, E.I. Franses, O.A. Bararan. J. Colloid and Interface Sci. 258 (2003) 310.
[12] J.K. Ferri, S.Y. Lin, K.J. Stebe. J. of Colloid and Interface Sci. 241 (2001) 154.
[13] S.-Y. Lin AIChE Journal. 36 (12) (1990) 1785.
[14] S.-Y. Lin, W.-J. Wang, C.-T. Hsu. Langmuir. 13 (1997) 6211.
[15] S.-Y. Lin, R.-Y. Tsay, L.-W. Lin, S.-I. Chen. Langmuir. 12 (1996) 6530.
[16] R.-Y. Tsay, S.-Y. Lin, L.-W. Lin, S.-I. Chen. Langmuir. 13 (1997) 3191.
[17] Y.-C. Lee, S.-Y. Lin, H.-S. Liu. Langmuir. 17 (2001) 6196.
[18] V.B. Fainerman, R. Miller, R. Wustneck, A.V. Makievski, J. Phys. Chem. 100 (1996) 7669.
[19] C. Chang, E.I. Franses. Colloids and Surfaces-A. 100 (1995) 1.
[20] P. Chen, A.W. Neumann. Colloids and Surfaces A. 143 (1998) 331.
[21] C.H. Chang, E.I. Franses, Colloids and Surfaces 69 (1993) 189.
[22] M.E. Biswas, I. Chatzis, M.A. Ioannidid, P. Chen, J. Colloid Interface Sci. 286 (2005) 14.
[23] H.-C. Chang, C.-T. Hsu, S.-Y. Lin. Langmuir. 14 (1998) 2476.
[24] gPRMOS Introductory user guide, Process Systems Enterprise Ltd., United Kingdom, 2001.
[25] Y.-C. Lee, Y.-B. Liou, R. Miller, H.-S. Liu, S.-Y. Lin. Langmuir. 18 (2002) 2686.
[26] R. Pan, J. Green, C. Maldarelli. J. Colloid and Interface Sci. 205 (1998) 213.